
Learning to Noise: Application-Agnostic Data Sharing with Local Differential Privacy

Alex Mansbridge¹ Gregory Barbour^{2*} Davide Piras^{2*} Christopher Frye² Ilya Feige² David Barber¹

Abstract

The collection and sharing of individuals' data has become commonplace in many industries. *Local differential privacy* (LDP) is a rigorous approach to preserving data privacy even from a database administrator, unlike the more standard *central* differential privacy. To achieve LDP, one traditionally adds noise directly to each data dimension, but for high-dimensional data the level of noise required for sufficient anonymization all but entirely destroys the data's utility. In this paper, we introduce a novel LDP mechanism that leverages representation learning to overcome the prohibitive noise requirements of direct methods. We demonstrate that, rather than simply estimating aggregate statistics of the privatized data as is the norm in LDP applications, our method enables the training of performant machine learning models. Unique applications of our approach include private novel-class classification and the augmentation of clean datasets with additional privatized features. Methods that rely on central differential privacy are not applicable to such tasks. Our approach achieves significant performance gains on these tasks relative to state-of-the-art LDP benchmarks that noise data directly.

1. Introduction

The collection of personal data is ubiquitous, and unavoidable for many in everyday life. The use of such data for training machine learning algorithms has become instrumental in improving the quality and user experience of many products and services. However, evidence of data misuse and data breaches (Sweeney, 1997; Jolly, 2020) has brought the concept of data privacy into sharp focus, fueling regulatory changes, as well as a shift in personal pref-

*Equal contribution ¹University College London & The Alan Turing Institute, London, UK ²Faculty, 54 Welbeck Street, London, UK. Correspondence to: Alex Mansbridge <amansbridge@turing.ac.uk>.

erences. The onus has now fallen on organizations to determine if they are willing and able to collect personal data under these changing expectations. There is thus a growing need for methods of data collection that preserve privacy while maintaining utility to improve products and services.

Often coined the 'gold standard' of privacy guarantees, *central differential privacy* (CDP) (Dwork et al., 2006) protects against an adversary determining the presence of an individual in a dataset. It provides a quantifiable definition that is robust to post-processing and composition (Dwork & Roth, 2014). The CDP framework relies on the calibrated addition of noise to the output of statistical queries on the dataset, so that the presence or absence of any individual in the dataset is undetectable.

In the context of machine learning, private optimization algorithms such as DP-SGD (Abadi et al., 2016), DP-Adam (Gylberth et al., 2017), and PATE (Papernot et al., 2017) add noise throughout training to produce models that are CDP with respect to their training data.

Recent work, often considered state-of-the-art in private data publishing, trains a generative model with a private optimization algorithm (Xie et al., 2018; Triastcyn & Faltings, 2019; Acs et al., 2019; Takagi et al., 2021). By sampling from such a model, one can construct a synthetic dataset that satisfies CDP with respect to the model's training data. For certain applications, this approach is powerful. However, it comes with a fundamental limitation: the induced synthetic data provides no information about the features of specific, real individuals.

The notion of *local differential privacy* (LDP) addresses this limitation (Kasiviswanathan et al., 2008; Duchi et al., 2013). LDP has its roots in the technique of randomized response (Warner, 1965) which preserves the privacy of survey respondents, granting them plausible deniability by only having them answer a sensitive binary question truthfully if a secret coin flip returns heads. Generalizing this idea, LDP provides a mathematically provable privacy guarantee for members of a database against both a potential adversary and the database administrator. For continuous data, Laplace-distributed noise (Dwork et al., 2006) is commonly used to impose LDP.

There are a number of LDP mechanisms for data collection and we review these in detail in Section 6. However, we note that even the ‘multi-dimensional’ mechanisms are only applied in low-dimensional settings. To our knowledge, no existing LDP techniques have shown compelling results on high-dimensional data. This “curse of dimensionality”, in which the noise added to each feature scales linearly with the data’s dimensionality, is a well-known issue in differential privacy (Zhang et al., 2017).

In this work, we leverage techniques from representation learning to overcome the limitation of current LDP mechanisms to low-dimensional data. To motivate our approach, consider the fact that it is often a good approximation to assume a given high-dimensional dataset lives on a much lower-dimensional manifold. Applying a general privatization mechanism to low-dimensional representations should thus enable us to *learn* how to add noise to the raw high-dimensional data efficiently.

Our work builds on generative latent variable modelling (Kingma & Welling, 2014; Rezende et al., 2014). In our model, sampling in latent space adds Laplace-distributed noise to a datapoint’s low-dimensional representation. Reconstructing a datapoint is then equivalent to efficiently adding complex, non-linear noise to its raw features to induce LDP. We refer to this novel technique as the variational Laplace mechanism (VLM). To train the VLM, we assume access to a clean, internal data set whose privacy should remain preserved, as is the case with the synthetic data generation methods discussed above.

Owing to the wealth of representation learning research on images (Gulrajani et al., 2017), audio (van den Oord et al., 2017), video (Denton & Fergus, 2018), and text (Bowman et al., 2016), the VLM can be easily adapted to many data domains. Moreover, our approach is application-agnostic: data privatized with VLM can be used for a broad range of downstream tasks.

In particular, we demonstrate that our approach achieves state-of-the-art performance on three major applications that existing CDP models cannot address:

- Privatized data is collected with the VLM and used to train downstream machine learning models, demonstrating state-of-the-art utility preservation on high dimensional data under LDP.
- The VLM can be used, without re-training, to collect distributionally-shifted data for model training. In particular, we train a classifier on privatized data for novel class classification.
- As a mechanism for LDP, the VLM can track the IDs of real individuals whilst privatizing their sensitive features. We use this to augment internal data with

privatized features from an external source to improve a classifier’s performance on the combined feature set.

2. Basic Definitions and Notation

To formalize the concept of differential privacy, we first introduce some definitions and notation.

Definition ((ϵ, δ)-central differential privacy): Let $\mathcal{A} : \mathcal{D} \rightarrow \mathcal{Z}$ be a randomized algorithm, that takes as input datasets from the dataset domain \mathcal{D} . We say \mathcal{A} is (ϵ, δ) -central differentially private if for $\epsilon, \delta \geq 0$, for all subsets $S \subseteq \mathcal{Z}$, and for all neighboring datasets $D, D' \in \mathcal{D}$, we have

$$p(\mathcal{A}(D) \in S) \leq e^\epsilon p(\mathcal{A}(D') \in S) + \delta \quad (1)$$

where for D and D' to be neighboring means that they are identical in all but one datapoint.

Intuitively, this states that one cannot tell (with a level of certainty determined by (ϵ, δ)) whether an individual is present in a database or not. When $\delta = 0$ we say \mathcal{A} satisfies ϵ -CDP.

While CDP relies on a trusted database administrator, LDP provides a much stricter guarantee in which the individual does not need to trust an administrator. Instead, individuals are able to privatize their data before sending it using a *local* randomized algorithm.

Definition ((ϵ, δ)-local differential privacy): A local randomized algorithm $\mathcal{A} : \mathcal{X} \rightarrow \mathcal{Z}$, that takes as input a datapoint from the data domain \mathcal{X} , satisfies (ϵ, δ) -local differential privacy if for $\epsilon, \delta \geq 0$, for all $S \subseteq \mathcal{Z}$, and for any inputs $x, x' \in \mathcal{X}$,

$$p(\mathcal{A}(x) \in S) \leq e^\epsilon p(\mathcal{A}(x') \in S) + \delta \quad (2)$$

When $\delta = 0$ we say \mathcal{A} satisfies ϵ -LDP.

Definition (Local ℓ_1 sensitivity): The ℓ_1 sensitivity of a function $f : \mathcal{X} \rightarrow \mathcal{Z}$, where $\mathcal{Z} \subseteq \mathbb{R}^k$, is defined as

$$\Delta f = \max_{x, x' \in \mathcal{X}} \|f(x) - f(x')\|_1 \quad (3)$$

Definition (Local Laplace mechanism): The local Laplace mechanism $\mathcal{M} : \mathcal{X} \rightarrow \mathbb{R}^k$ is a randomized algorithm defined as

$$\mathcal{M}(x, f(\cdot), \epsilon) = f(x) + (s_1, \dots, s_k) \quad (4)$$

for $x \in \mathcal{X}$, $s_i \sim \text{Laplace}(0, \Delta f / \epsilon)$, and some transformation function $f : \mathcal{X} \rightarrow \mathcal{Z}$ with local ℓ_1 sensitivity Δf .

The local Laplace mechanism satisfies ϵ -LDP (see Appendix A for proof).

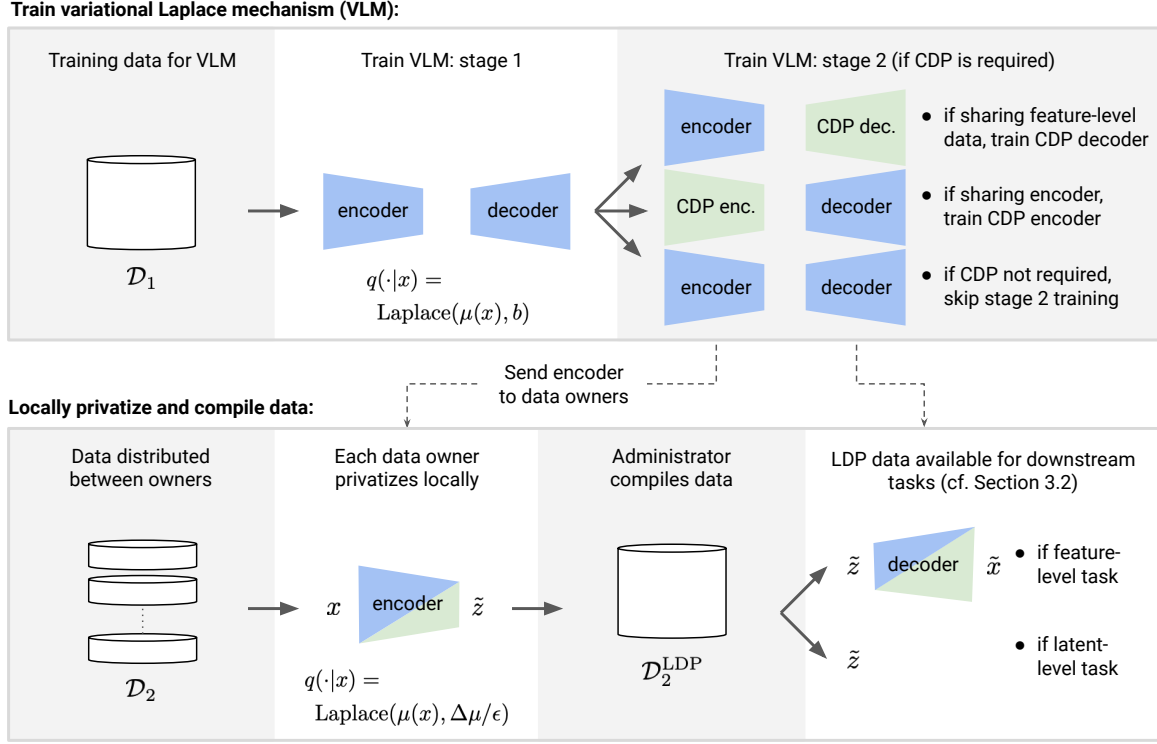


Figure 1. Schematic diagram of VLM training (top) and local data privatization and collection (bottom), as outlined in Section 3.1. Green shading indicates parameters satisfying CDP with respect to the training set.

3. Proposed Method

Many existing local mechanisms noise each feature independently; by the composition theorem (Dwork & Roth, 2014), the i^{th} feature contributes towards the overall LDP guarantee of the d -dimensional datapoint as $\epsilon = \sum_{i=1}^d \epsilon_i$. Clearly as d increases, ϵ_i decreases for each feature i and the noise required to induce ϵ -LDP thus grows with data dimensionality. For high-dimensional datasets like images or large tables, features are often highly correlated; consequently, noising features independently is wasteful towards privatizing the information content in each datapoint. A more effective approach is to learn a generic, application-agnostic mechanism that adds complex, non-linear noise via a mapping to a lower-dimensional data manifold.

To this end, we train a generative latent-variable model to learn a low-dimensional latent representation of our data. This learned mapping from data space to latent space forms our function $f(\cdot)$ in Equation 4. Applying the Laplace mechanism (as described in Section 3.1) thus ensures the encoded latents, and indeed reconstructed datapoints, satisfy LDP. We can therefore privatize data at the latent level or original-feature level; preference between these two options is application specific, and we investigate both experimentally. $f(\cdot)$ is trained using a separate, unlabelled dataset from a similar distribution, which most organiza-

tions will typically already have access to. We assume in our experiments that this unlabelled dataset is internal and sensitive, though it could also be a public dataset. The privacy of this internal dataset is guaranteed under CDP.

Data owners can apply this learned LDP mechanism to their data before sharing with the database administrator, who then forms an LDP data set from the collected data. This set, along with information on the type of noise added, can be used very broadly; we consider training downstream machine learning algorithms as our evaluative downstream task. Though our privatization method is task agnostic, in this paper we focus on classification tasks in which some features x are used to predict the corresponding label y . At inference time, it is shown that this classifier can act on either clean or privatized datapoints, depending on the application.

3.1. Learning a Laplace Mechanism

We assume that our data x is generated by a random process involving a latent variable z . We then optimize a lower bound on the log likelihood (Kingma & Welling, 2014)

$$\log p(x) = \log \int p(z)p_\theta(x|z)dz \quad (5)$$

$$\geq \mathbb{E}_{q_\phi(z|x)} [\log p_\theta(x|z)] - D_{\text{KL}}(q_\phi(z|x) || p(z)) \quad (6)$$

where $p(z)$ is the prior distribution and $q_\phi(z|x)$ is the approximate posterior over the latent. The generative distribution $p_\theta(x|z)$ and approximate inference distribution $q_\phi(z|x)$ are parameterized by neural networks, with learnable parameters θ and ϕ respectively. While the distributions over latent space are commonly modeled as Gaussian, we aim to learn a Laplace mechanism and so instead we choose

$$p(z) = \prod_{i=1}^d p(z_i) \quad \text{and} \quad q_\phi(z|x) = \prod_{i=1}^d q_\phi(z_i|x) \quad (7)$$

using Laplace distributions $p(z_i) = \text{Laplace}(0, 1/\sqrt{2})$ and $q_\phi(z_i|x) = \text{Laplace}(\mu_\phi(x)_i, b)$.

We parameterize $\mu_\phi(\cdot)$ with a neural network and restrict its output via a carefully chosen activation function $\nu(\cdot)$ acting on the final layer $\mu_\phi(\cdot) = \nu(h_\phi(\cdot))$, where

$$\nu(y) = \begin{cases} \frac{yl}{\|y\|_1} & \text{if } \|y\|_1 > l \\ y & \text{otherwise.} \end{cases} \quad (8)$$

This ensures $\Delta\mu_\phi = 2l$. If the scale is fixed to $b = 2l/\epsilon_x$, drawing a sample \tilde{z} from the encoder distribution $q_\phi(z|x)$ is equivalent to passing a point x through the local Laplace mechanism $\mathcal{M}(x, \mu_\phi(\cdot), \epsilon_x)$ from Equation 4. Thus, \tilde{z} is a representation of x that satisfies ϵ_x -LDP. We refer to this method as the variational Laplace mechanism (VLM).

We further prove in Appendix B that a reconstruction \tilde{x} obtained by passing \tilde{z} through the decoder network $p_\theta(\cdot|z)$ also satisfies ϵ_x -LDP, allowing us to privatize datapoints at either latent level \tilde{z} , or original-feature level \tilde{x} .

Note that b is always fixed at inference (i.e. data privatization) time to guarantee \tilde{z} is ϵ_x -LDP. However, we experiment with learning b during training, as well as fixing it to different values.

Certain applications of our method require us to share either the encoder or decoder of the VLM at inference time. If the VLM training data itself contains sensitive information, then the part of the network that gets shared must satisfy CDP with respect to this training data. We found the following two-stage VLM training approach to be helpful in these cases:

- **Stage 1:** Train a VLM with encoding distribution $q_\phi(z|x)$ and decoding distribution $p_\theta(x|z)$ using a non-DP optimizer, such as Adam (Kingma & Ba, 2015).
- **Stage 2:** If training a DP-encoder model, fix θ , and retrain the encoder with a new distribution $q_{\phi_{\text{private}}}(z|x)$. If training a DP-decoder, fix ϕ and replace the decoder with $p_{\theta_{\text{private}}}(x|z)$. Optimize ϕ_{private} or θ_{private} as appropriate using DP-Adam (Gylberth et al., 2017).

Section 4 and Appendix D outline applications in which private VLM components are required. Full details of the VLM training, as well as the data collection and privatization process, are shown in Figure 1.

3.2. Training Classifiers on Private Data

For supervised learning we must also privatize a target y . In this paper we train a classifier and so $y \in \{1, \dots, K\}$ is a discrete scalar. To obtain a private label \tilde{y} , we flip y with some fixed probability $p < (K-1)/K$ to one of the other $K-1$ categories: $p(\tilde{y} = i|y = j) = (1-p)\mathbb{I}(i = j) + p/(K-1)\mathbb{I}(i \neq j)$. Setting $p = (K-1)/(e^{\epsilon_y} + K-1)$ induces ϵ_y -LDP (see Appendix C for proof). For problems such as regression, $y \in \mathbb{R}$ may be a continuous scalar, and one could privatize this with e.g. the Laplace Mechanism.

By the composition theorem (Dwork & Roth, 2014), the tuple (\tilde{x}, \tilde{y}) satisfies ϵ -LDP where $\epsilon = \epsilon_x + \epsilon_y$. Downstream models may be more robust to label noise than feature noise, or vice versa, so for a fixed ϵ we set $\epsilon_x = \lambda\epsilon$ and $\epsilon_y = (1-\lambda)\epsilon$, with λ chosen to maximise the utility of the dataset. In practice, we treat λ as a model hyperparameter.

Rather than training the classifier $p_\psi(\cdot)$ directly on private labels, we incorporate the known noise mechanism into our objective function

$$\log p(\tilde{y}|\tilde{x}) = \log \sum_{y=1}^K p(\tilde{y}|y) p_\psi(y|\tilde{x}) \quad \text{or} \quad (9)$$

$$\log p(\tilde{y}|\tilde{z}) = \log \sum_{y=1}^K p(\tilde{y}|y) p_\psi(y|\tilde{z}) \quad (10)$$

depending on whether we choose to work on a feature level, or latent level.

At inference time we can classify privatized points using $p_\psi(y|\tilde{x})$ or $p_\psi(y|\tilde{z})$. We will also show empirically that we can classify clean points using the same classifier. We refer to these tasks as *private* and *clean* classification, with real-world applications given in Sections 4 and 5.

3.3. Private Validation and Hyper-parameter Optimization

Typically for model validation, one needs access to clean labels y (and clean data x for validating a clean classifier). However, we note that we need only collect privatized model performance metrics on test and validation sets, rather than actually collect the raw datapoints.

To do this, we send the trained classifier to members of a validation set so that they can test whether it classified correctly: $c \in \{0, 1\}$. They return an answer, flipped with probability $p = 1/(e^\epsilon + 1)$ such that the flipped answer \tilde{c} satisfies ϵ -LDP, and we can estimate the true validation set

accuracy $A = \frac{1}{N_{\text{val}}} \sum_{n=1}^{N_{\text{val}}} c_n$ from the privatized accuracy $\tilde{A} = \frac{1}{N_{\text{val}}} \sum_{n=1}^{N_{\text{val}}} \tilde{c}_n$ using

$$A = \frac{\tilde{A} - p}{1 - 2p} \quad (11)$$

(Warner, 1965). We use this method to implement a grid search over hyperparameters of our model.

3.4. Benchmarks

We benchmark against two mechanisms that noise each feature independently: the traditional Laplace mechanism, and Wang et al. (2019)’s piecewise mechanism (along with a flip mechanism for categorical tabular features). Further details on these benchmarks can be found in Section 6.

Since we have no prior knowledge about which features are most important, we choose the noise level for each feature to be such that $\epsilon_i = \epsilon/d$. See Appendix E.2 for further experimental details on these benchmarks.

4. Classifying Clean Datapoints: Applications and Experiments

Below we demonstrate the versatility of our method by outlining a non-exhaustive list of potential real-world-inspired applications, with corresponding experiments. Experiments are trained on the MNIST dataset (LeCun et al., 1998), or the Lending Club dataset¹. The CDP requirements differ between applications, but are explicitly stated for each application in Appendix D. For all stated $(\epsilon_{\text{central}}, \delta_{\text{central}})$ -CDP results we use $\delta_{\text{central}} = 10^{-5}$, whilst for $(\epsilon_{\text{local}}, \delta_{\text{local}})$ -LDP results, $\delta_{\text{local}} = 0$. All results quoted are the mean of 3 trials; error bars represent ± 1 standard deviation. Appendix E describes experimental setup and dataset information.

In Sections 4.1 and 4.2, we investigate the *clean* classification task, and report on *clean* accuracy. Namely, the classifiers are trained on privatized data in order to classify clean datapoints at inference time. We also study the classification of privatized datapoints, using a classifier trained on privatized data, which we refer to as *private* classification (and report *private* accuracy) in Section 5.

4.1. Data Collection

Organizations may have access to some (potentially unlabelled) clean, internal data \mathcal{D}_1 , but want to collect additional privatized, labelled data \mathcal{D}_2 in order to train a machine learning algorithm. For example, a public health body may have access to some medical images, but want

to train a diagnosis classifier to be used in hospitals, using labelled data collected privately from their patients. Similarly, a tech company with access to some user data may want to collect private, labelled training data from a broader group of users to train a classifier for use in a mobile app. Finally, a multinational company may be allowed to collect raw data on their US users, but only LDP data on users from countries with more restrictive data privacy laws.

As in Sections 3.1 - 3.3, we first train a VLM with a DP encoder using \mathcal{D}_1 , then privatize all datapoints and corresponding labels in \mathcal{D}_2 before training a classifier with this privatized training set. In this experiment, we assume the data \mathcal{D}_1 and \mathcal{D}_2 follow the same data distribution, however in practice this may not always be the case. For example, when \mathcal{D}_2 is sales data collected in a different time period, or user data collected in a different region, we may expect the distribution to change. We have omitted such an experiment here, but the extreme case of this distributional shift is explored experimentally in Section 4.2.

We run this experiment on both MNIST and Lending Club, with data splits outlined in Appendix E.1.1. We significantly outperform the two benchmarks in all experiments, with results shown in Figure 2. For MNIST, both benchmarks performed at random accuracy for all local $\epsilon \leq 100$. For Lending Club, the Laplace benchmark performed at random accuracy for all local $\epsilon \leq 20$, while Wang et al. (2019)’s performed slightly above random at $\epsilon = 6$ (though random performance is within error bars for $\epsilon \leq 8$). Our method performed above random for all local $\epsilon \geq 1$.

For MNIST, we see that latent-level classification outperforms feature-level classification for higher local- ϵ values. Indeed, the data processing inequality states we cannot gain more information about a given datapoint by passing it through our decoder. However at lower local ϵ , we see this gap in performance diminish. We hypothesize that at this point, so much noise is added to the latent that the latent level classifier struggles, while on pixel level the VLM decoder improves classification by adding global dataset information from \mathcal{D}_1 to the privatized point.

For Lending Club, we see little difference between latent-level and feature-level accuracy. However we also note that the features are not as highly correlated as in MNIST, so perhaps the decoder has less influence on results.

Finally, we see that reducing central ϵ has an adverse effect on MNIST classification accuracy, especially for higher local ϵ . The effect seems negligible for Lending Club and we hypothesize that this is due to the large quantity of training data, along with the easier task of binary classification.

¹<https://www.kaggle.com/wordsforthewise/lending-club>

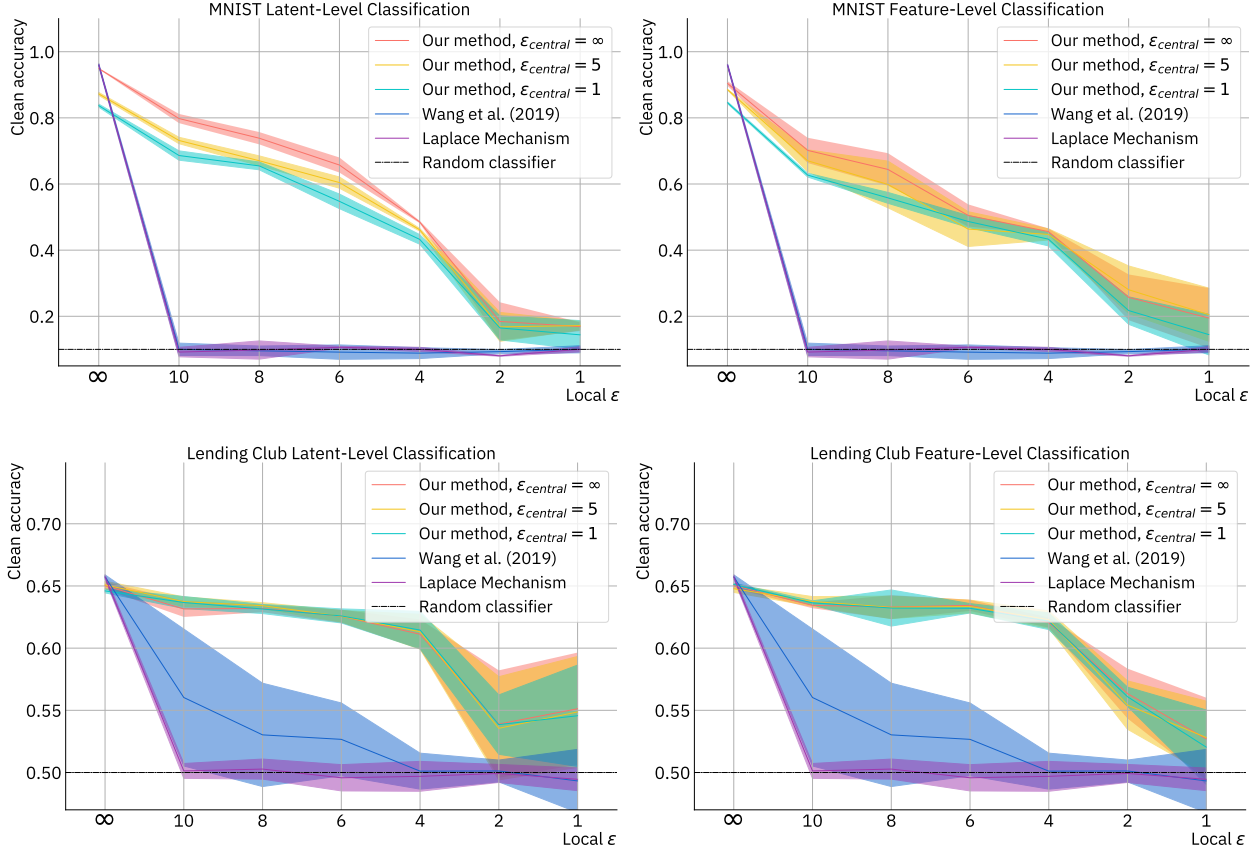


Figure 2. Clean accuracy as a function of local ϵ for data collection. Results are shown for the MNIST dataset (top) and Lending Club (bottom), on latent level (left) and feature level (right). Each line indicates a different value of $(\epsilon, \delta = 10^{-5})$ -CDP at which the encoder was trained. The x -axis shows the ϵ -LDP guarantee for the collected training set.

4.2. Novel-Class Classification

As discussed in Section 4.1, the internal data \mathcal{D}_1 and the data to be collected \mathcal{D}_2 , may follow different data distributions. In the extreme case, the desired task on \mathcal{D}_2 may be to predict membership in a class that is not even present in dataset \mathcal{D}_1 . For example, in a medical application there may be a large existing dataset \mathcal{D}_1 of chest scans, but only a relatively small dataset \mathcal{D}_2 that contains patients with a novel disease. As before, a public health body may want to train a novel-disease classifier to distribute to hospitals. Similarly, a software developer may have access to an existing dataset \mathcal{D}_1 , but want to predict software usage data for \mathcal{D}_2 , whose label is specific to the UI of a new release.

We run this experiment on MNIST, where the internal \mathcal{D}_1 contains training images from classes 0 to 8, (with a small number of images held out for classification), and \mathcal{D}_2 contains all training images from class 9. As in Sections 3.1 and 3.2, we first train a VLM with a DP encoder on \mathcal{D}_1 , then privatize all images in \mathcal{D}_2 (we are not required to collect or privatize the label since all images have the same label). We then train a binary classifier on the dataset formed

of the private 9's and the held out internal images from classes 0-8 (which we privatize and label 'not 9's').

Results are shown in Figure 3. On both latent and feature level, we obtain approximately 75% accuracy at local $\epsilon = 2$ and above random performance at local $\epsilon = 1$. Again, both benchmarks achieve random performance for all local $\epsilon \leq 100$ (not shown in the figure). As before, the effects of reducing central ϵ appear greater at higher local ϵ values, and we see that the latent-level classifier outperforms the feature-level classifier at high local ϵ , but not at low local ϵ .

4.3. Data Joining

An organization training a classifier on some labelled dataset \mathcal{D}_1 could potentially improve performance by augmenting their dataset with other informative features, and so may want to join \mathcal{D}_1 with features from another dataset \mathcal{D}_2 . We assume the owner of \mathcal{D}_2 may only be willing to share a privatized version of this dataset. For example, two organizations with mutual interests, such as the IRS and a private bank, or a fitness tracking company and a hospital, may want to join datasets to improve the performance of

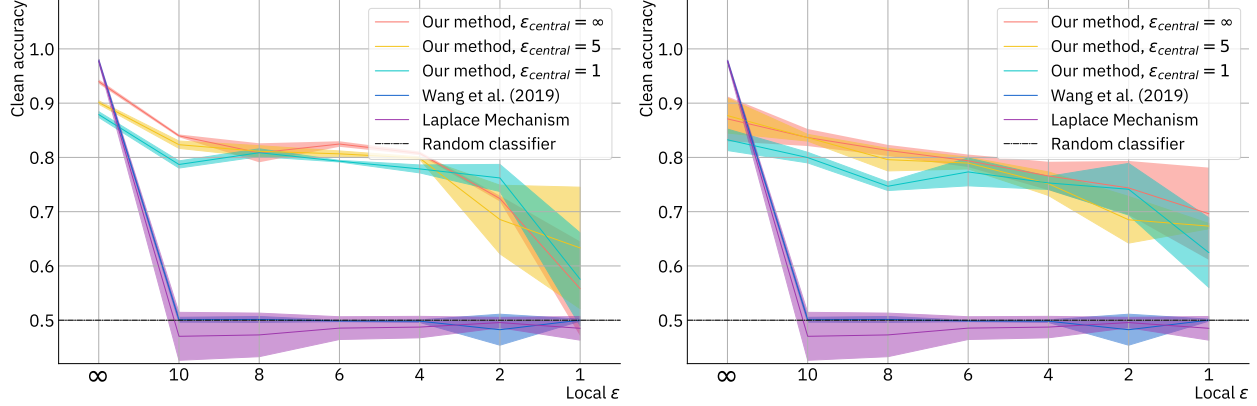


Figure 3. Clean accuracy as a function of local ϵ for novel-class classification on latent level (left) and feature level (right). Each line indicates a different value of $(\epsilon, \delta = 10^{-5})$ -CDP at which the encoder was trained. The x -axis shows the ϵ -LDP guarantee for the collected training set.

their algorithm. Similarly, it may be illegal for multinational organizations to share and join non-privatized client data between departments in different regions, but legal to do so when the shared data satisfies LDP.

We run this experiment on Lending Club, where we divide the dataset slightly differently from previous experiments: both datasets contain all rows, but \mathcal{D}_1 contains a subset of (clean) features, along with the clean label, and \mathcal{D}_2 contains the remaining features (to be privatized).

We follow a privatization procedure similar to that of Section 3.1, with the distinction that the VLM should be both trained on \mathcal{D}_2 , and used to privatize \mathcal{D}_2 . For the classification problem, instead of Equation 10, we optimize $\log p_\psi(y_1|x_1, \tilde{x}_2)$ where $(x_1, y_1) \in \mathcal{D}_1$ and $\tilde{x}_2 \in \mathcal{D}_2^{(\text{private})}$. We are not required to conduct a private grid search over hyperparameters as in Section 3.3, since we have access to all raw data needed for validation. Note that unlike the previous two experiments, we train the classifier on a combination of both clean and privatized features, and we classify this same ‘semi-private’ group of features at inference time.

Results are shown in Figure 4. We can see that using features from \mathcal{D}_1 only, we obtain classification accuracy of 56.1%, while classifying on all (clean) features, we obtain 65.8% accuracy. Neither benchmark achieves more than 1 percentage point accuracy increase over classifying the clean features only, whereas our method achieves a significant improvement for local $\epsilon \in [4, 10]$. We share the privatized features on latent level in this experiment and so do not need to satisfy CDP.

5. Classifying Private Datapoints: Applications and Experiments

In Sections 4.1 and 4.2, we have been investigating the use of privatized training data to train algorithms that classify

clean datapoints. In some use cases however, we may want to train algorithms that act directly on LDP datapoints at inference time. Most notably, in the data collection framework, the organization may want to do inference on individuals whose data they have privately collected.

However from the definition of LDP in Equation 2, it is clear that a considerable amount of information about a datapoint x is lost after privatization, and in fact, classification performance is fundamentally limited. In Appendix F, we show that for a given local ϵ , the accuracy A of a K -class latent-level classifier acting on a latent representation (of dimension $d \geq K/2$) privatized with the local Laplace mechanism is upper bounded by

$$A \leq \sum_{j=0, j \neq 1}^{K/2-1} \left(\binom{K/2-1}{j} \frac{(-1)^j}{1-j} \left[\frac{e^{-j\epsilon/2}}{1+j} - \frac{e^{-\epsilon/2}}{2} \right] \right) - \frac{\epsilon+1}{8} (K-2) e^{-\epsilon/2} \quad (12)$$

In Figure 5, we show the accuracy of our method from Section 4.1 (data collection) when applied to privatized datapoints at inference time, and compare to the upper bound in Equation 12.

Running this experiment on MNIST, we see a considerable drop in performance when classifying privatized datapoints, compared with clean classification results.

We are clearly not saturating the bound from Equation 12. While it may initially appear that our method is underperforming, we note that our method aims to build a downstream-task-agnostic privatized representation of the data. This means that the representation must contain more information than just the class label. Meanwhile, the upper bound is derived from the extreme setting in which the latent encodes only class information, and would be unable to solve any other downstream task.

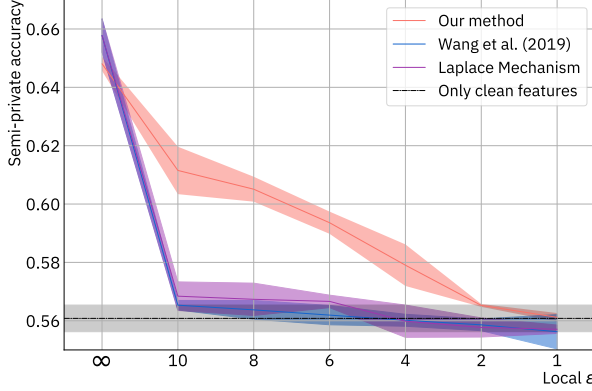


Figure 4. ‘Semi-private’ accuracy versus local ϵ for data joining (private features shared and joined on latent level). The x -axis shows the ϵ -LDP guarantee for the collected training set.

Though Equation 12 is constructed under the framework of latent-level classification, we do note that our feature-level classifier seems to marginally outperform the latent-level one (see Appendix G). This may be a result of the decoder de-noising the latent to some extent.

6. Related Work

Many of the existing LDP techniques were developed for specific tasks: Ding et al. (2017) study the repeated collection of one-dimensional telemetry data for mean and histogram estimation. Erlingsson et al. (2014) develop a technique for collecting aggregate statistics on categorical attributes, with Fanti et al. (2016) extending this to model correlations between dimensions. Ren et al. (2018) discuss the poor performance of these models on high dimensional data and instead estimate the distribution of collected data from which they sample a synthetic dataset; though the stricter LDP guarantees are satisfied, the range of applications is limited as with CDP synthetic generation above. We note that their method results in a high communication cost between the data collector and individuals.

For the general collection of continuous (one-dimensional) attributes, the Laplace mechanism (Dwork et al., 2006) is commonly used. More recently, Duchi et al. (2018) and Wang et al. (2019) introduced lower-variance mechanisms for continuous one-dimensional attributes. They also introduce mechanisms for multidimensional data, with Wang et al. (2019)’s able to handle both categorical and continuous attributes. However these methods do not easily scale to the high-dimensionality of modern machine learning datasets: Duchi et al. (2018)’s mechanism involves a large constant that scales with data dimension d , while Wang et al. (2019)’s mechanism involves sending only $k \ll d$ attributes (where for our experiments $k \leq 4$).

We therefore benchmark against methods in which one-

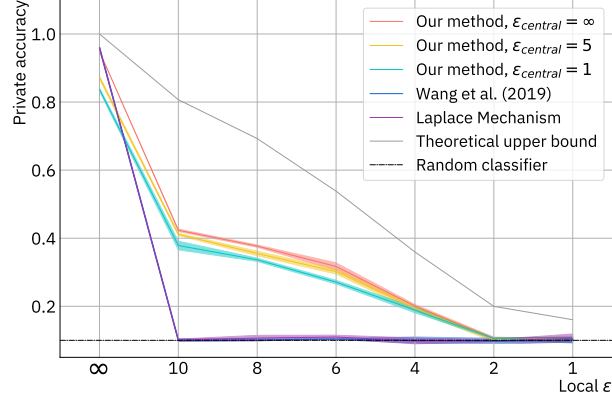


Figure 5. Private accuracy versus local ϵ for latent-level data collection. Each line indicates a different value of $(\epsilon, \delta = 10^{-5})$ -CDP at which the encoder was trained. The x -axis shows the ϵ -LDP guarantee for the collected training set.

dimensional mechanisms are applied to all features independently. We experiment with the Laplace mechanism, Duchi et al. (2018)’s mechanism and Wang et al. (2019)’s piecewise mechanism for continuous features (and use a flip mechanism for categorical tabular features). We noticed little difference between Duchi et al. (2018)’s and the piecewise mechanism, and so have shown only results for the piecewise mechanism and Laplace mechanism in our experiments.

As with our approach, these benchmark mechanisms can act on any data type, and form a downstream-task-agnostic LDP version of the data.

7. Conclusion and Future Work

In this paper we have introduced a framework for collecting and sharing data under the strict guarantees of LDP. We induce LDP by learning to efficiently add noise to any data type for which representation learning is possible. We have demonstrated a number of different applications of our framework, spanning important issues such as medical diagnosis, financial crime detection, and customer experience improvement, significantly outperforming existing baselines on each of these.

This is the first use of latent-variable models for learning LDP mechanisms. We foresee that even stronger performance could be achieved by combining our method with state-of-the-art latent-variable models that utilise more complex architectures, and often deep hierarchies of latents (Gulrajani et al., 2017; Maaløe et al., 2019; Ho et al., 2019). In this work we sought to show that significant hurdles in LDP for high-dimensional data could be overcome using a representation-learning driven randomization algorithm, which we have indeed demonstrated.

References

Abadi, M., Chu, A., Goodfellow, I., McMahan, H. B., Mironov, I., Talwar, K., and Zhang, L. Deep learning with differential privacy. In *Proceedings of the 2016 ACM SIGSAC Conference on Computer and Communications Security*, 2016.

Acs, G., Melis, L., Castelluccia, C., and De Cristofaro, E. Differentially private mixture of generative neural networks. *IEEE Transactions on Knowledge and Data Engineering*, 2019.

Bowman, S. R., Vilnis, L., Vinyals, O., Dai, A., Jozefowicz, R., and Bengio, S. Generating sentences from a continuous space. In *Conference on Computational Natural Language Learning*, 2016.

Denton, E. and Fergus, R. Stochastic video generation with a learned prior. In *International Conference on Machine Learning*, 2018.

Ding, B., Kulkarni, J., and Yekhanin, S. Collecting telemetry data privately. In *Advances in Neural Information Processing Systems 30*. 2017.

Duchi, J. C., Jordan, M. I., and Wainwright, M. J. Local privacy and statistical minimax rates. In *IEEE 54th Annual Symposium on Foundations of Computer Science*, 2013.

Duchi, J. C., Jordan, M. I., and Wainwright, M. J. Minimax optimal procedures for locally private estimation. In *Journal of the American Statistical Association*, 2018.

Dwork, C. and Roth, A. The algorithmic foundations of differential privacy. In *Foundations and Trends in Theoretical Computer Science*, 2014.

Dwork, C., McSherry, F., Nissim, K., and Smith, A. Calibrating noise to sensitivity in private data analysis. In *Theory of Cryptography*, 2006.

Erlingsson, Ú., Pihur, V., and Korolova, A. RAPPOR: Randomized aggregatable privacy-preserving ordinal response. In *Proceedings of the 2014 ACM SIGSAC Conference on Computer and Communications Security*, 2014.

Fanti, G., Pihur, V., and Erlingsson, Ú. Building a RAPPOR with the unknown: Privacy-preserving learning of associations and data dictionaries. *Proceedings on Privacy Enhancing Technologies (PoPETS)*, 2016.

Gulrajani, I., Kumar, K., Ahmed, F., Taiga, A. A., Visin, F., Vazquez, D., and Courville, A. PixelVAE: A latent variable model for natural images. In *International Conference on Learning Representations*, 2017.

Gylberth, R., Adnan, R., Yazid, S., and Basaruddin, T. Differentially private optimization algorithms for deep neural networks. In *International Conference on Advanced Computer Science and Information Systems (ICACSIS)*, 2017.

Ho, J., Chen, X., Srinivas, A., Duan, Y., and Abbeel, P. Flow++: Improving flow-based generative models with variational dequantization and architecture design. In *International Conference on Machine Learning*, 2019.

Jolly, J. FCA admits revealing confidential details of 1,600 consumers. In *The Guardian*, 2020.

Kasiviswanathan, S. P., Lee, H. K., Nissim, K., Raskhodnikova, S., and Smith, A. What can we learn privately? In *49th Annual IEEE Symposium on Foundations of Computer Science*, 2008.

Kingma, D. P. and Ba, J. Adam: A method for stochastic optimization. In *International Conference on Learning Representations*, 2015.

Kingma, D. P. and Welling, M. Auto-encoding variational Bayes. In *International Conference on Learning Representations*, 2014.

LeCun, Y., Bottou, L., Bengio, Y., and Haffner, P. Gradient-based learning applied to document recognition. *Proceedings of the IEEE*, 1998.

Maaløe, L., Fraccaro, M., Liévin, V., and Winther, O. BIVA: A very deep hierarchy of latent variables for generative modeling. In *Advances in Neural Information Processing Systems 32*. 2019.

Papernot, N., Abadi, N., Erlingsson, U., Goodfellow, I., and Talwar, K. Semi-supervised knowledge transfer for deep learning from private training data. In *International Conference on Learning Representations*, 2017.

Ren, X., Yu, C., Yu, W., Yang, S., Yang, X., McCann, J. A., and Yu, P. S. LoPub: High-dimensional crowdsourced data publication with local differential privacy. In *IEEE Transactions on Information Forensics and Security*, 2018.

Rezende, D. J., Mohamed, S., and Wierstra, D. Stochastic backpropagation and approximate inference in deep generative models. In *International Conference on Machine Learning*, 2014.

Sweeney, L. Weaving technology and policy together to maintain confidentiality. In *The Journal of Law, Medicine & Ethics*, 1997.

Takagi, S., Takahashi, T., Cao, Y., and Yoshikawa, M. P3GM: Private high-dimensional data release via privacy

preserving phased generative model. In *IEEE International Conference on Data Engineering*, 2021.

Triastcyn, A. and Faltings, B. Generating artificial data for private deep learning. In *Proceedings of the PAL: Privacy-Enhancing Artificial Intelligence and Language Technologies, AAAI Spring Symposium Series*, 2019.

van den Oord, A., Vinyals, O., and Kavukcuoglu, K. Neural discrete representation learning. In *Advances in Neural Information Processing Systems 30*, 2017.

Wang, N., Xiao, X., Yang, Y., Zhao, J., Hui, S. C., Shin, H., Shin, J., and Yu, G. Collecting and analyzing multi-dimensional data with local differential privacy. In *2019 IEEE 35th International Conference on Data Engineering (ICDE)*, 2019.

Warner, S. L. Randomized response: A survey technique for eliminating evasive answer bias. *Journal of the American Statistical Association*, 1965.

Xie, L., Lin, K., Wang, S., Wang, F., and Zhou, J. Differentially private generative adversarial network. *arXiv preprint, arXiv:1802.06739*, 2018.

Zhang, J., Cormode, G., Procopiuc, C. M., Srivastava, D., and Xiao, X. PrivBayes: Private data release via Bayesian networks. 2017.

A. Proof that the Local Laplace Mechanism Satisfies LDP

Claim: The local Laplace mechanism satisfies ϵ -local differential privacy.

Proof: We follow an approach similar to the proof in Dwork & Roth (2014) that the Laplace Mechanism satisfies CDP. Assume x and x' are two arbitrary datapoints. Denote $\mathcal{M}(x) = f(x) + (s_1, \dots, s_k)$ where $s_i \sim \text{Laplace}(0, \Delta f/\epsilon)$. Then for some arbitrary c we know that

$$\frac{p(\mathcal{M}(x) = c)}{p(\mathcal{M}(x') = c)} = \prod_{i=1}^k \frac{p(\mathcal{M}_i(x) = c_i)}{p(\mathcal{M}_i(x') = c_i)} \quad (13)$$

$$= \prod_{i=1}^k \frac{e^{-\frac{\epsilon|f_i(x) - c_i|}{\Delta f}}}{e^{-\frac{\epsilon|f_i(x') - c_i|}{\Delta f}}} \quad (14)$$

$$= \prod_{i=1}^k e^{\frac{\epsilon(|f_i(x') - c_i| - |f_i(x) - c_i|)}{\Delta f}} \quad (15)$$

$$\leq \prod_{i=1}^k e^{\frac{\epsilon|f_i(x') - f_i(x)|}{\Delta f}} \quad (16)$$

$$= e^{\frac{\epsilon||f(x') - f(x)||_1}{\Delta f}} \quad (17)$$

$$\leq e^\epsilon \quad (18)$$

where the first inequality comes from the triangle inequality, and the second comes from the definition of Δf .

B. Proof that Decoded Private Latents Satisfy LDP

Claim: If a point in latent space satisfies ϵ -LDP, then this point still satisfies ϵ -LDP after being passed through a deterministic function, such as the function that parameterizes the mean of the decoder network.

Proof: We follow an approach similar to the proof that central differential privacy is immune to post-processing (Dwork & Roth, 2014). Let $\mathcal{A} : \mathcal{X} \rightarrow \mathcal{Z}$ be a randomized algorithm that satisfies ϵ -LDP and $g : \mathcal{Z} \rightarrow \mathcal{Z}'$ be an arbitrary deterministic mapping. Let $S \subseteq \mathcal{Z}'$ and $T = \{z \in \mathcal{Z} : g(z) \in S\}$. Then

$$p(g(\mathcal{A}(x)) \in S) = p(\mathcal{A}(x) \in T) \quad (19)$$

$$\leq e^\epsilon p(\mathcal{A}(x') \in T) \quad (20)$$

$$= e^\epsilon p(g(\mathcal{A}(x')) \in S) \quad (21)$$

C. Proof that the Flip Mechanism Satisfies LDP

Claim: The flip mechanism $p(\tilde{y} = i|y = j) = (1-p)\mathbb{I}(i = j) + p/(K-1)\mathbb{I}(i \neq j)$ where $p = (K-1)/(e^\epsilon + K-1)$

satisfies ϵ -local differential privacy.

Proof: We can write, for any i, j, j' :

$$\frac{p(\tilde{y} = i|y = j)}{p(\tilde{y} = i|y = j')} = \frac{(1-p)\mathbb{I}(i = j) + p/(K-1)\mathbb{I}(i \neq j)}{(1-p)\mathbb{I}(i = j') + p/(K-1)\mathbb{I}(i \neq j')} \quad (22)$$

$$= \begin{cases} \frac{(K-1)(1-p)}{p} & i = j, i \neq j' \\ \frac{p}{(K-1)(1-p)} & i \neq j, i = j' \\ 1 & \text{otherwise} \end{cases} \quad (23)$$

$$= \begin{cases} e^\epsilon & i = j, i \neq j' \\ e^{-\epsilon} & i \neq j, i = j' \\ 1 & \text{otherwise} \end{cases} \quad (24)$$

Therefore, we have that for any i, j, j' , $\frac{p(\tilde{y}=i|y=j)}{p(\tilde{y}=i|y=j')} \leq e^\epsilon$.

D. Implementation Requirements for Different Applications

Table 1. Central differential privacy requirements for the VLM, with respect to the dataset \mathcal{D}_1 .

Application	Data Shared	CDP Requirement
Data Collection	Feature or latent level	DP-Encoder
Data Joining	Feature level	DP-Decoder
Data Joining	Latent level	None
Novel-Class Classification	Feature or latent level	DP-Encoder

In the scenario that \mathcal{D}_1 contains sensitive information, the encoder or decoder may need to be trained with the two-stage approach (outlined in Section 3.1) in order to guarantee (ϵ, δ) -CDP with respect to \mathcal{D}_1 . There are broadly two scenarios in which this is the case. Firstly, if private data is published on pixel level then a DP decoder is required. Secondly, if the encoder needs to be shared with the client (for example, in client side data collection) then a DP encoder is required. For pixel level data collection a DP decoder is not required, since the client can share their privatized latents and these can be ‘decoded’ to pixel level on the server side, avoiding the need to share the decoder. Table 1 explicitly outlines the CDP requirements for the applications discussed in our paper.

E. Experimental Set Up

For every experiment in the paper, we conducted three trials, and calculate the mean and standard deviation of accuracy for each set of trials. The error bars represent one standard deviation above and below the mean.

We use the MNIST dataset and the Lending Club dataset. MNIST is a dataset containing 70,000 images of handwritten digits from 0-9 with corresponding class labels; the task is 10-way classification to determine the digit number. Lending Club is a tabular, financial dataset made up of around 540,000 entries with 23 continuous and categorical features (after pre-processing, before one-hot encoding); the task is binary classification, to determine whether a debt will be re-paid.

E.1. Data Pre-Processing

For MNIST, we converted the images into values between 0 and 1 by dividing each pixel value by 255. These are then passed through a logit and treated as continuous.

For Lending Club, a number of standard pre-processing steps are performed, including:

- Dropping features that contain too many missing values, and those that would not normally be available to a loan company.
- Mean imputation to fill remaining missing values.
- Standard scaling of continuous features. Extreme outliers (those with features more than 10 standard deviations from the mean) are removed here.
- Balancing the target classes by dropping the excess class 0 entries.
- One-hot encoding categorical variables.

The target variable denotes whether the loan has been charged off or not, resulting in a binary classification task. The train, validation, test split is done chronologically according to the feature ‘issue date’.

In real world applications the sizes of the VLM training and validation sets, and the classifier training and validation sets would be pre-determined. For our experiments we used the data splits outlined in the following sections.

E.1.1. DATA COLLECTION

MNIST: The MNIST dataset contains 60,000 training points and 10,000 test points. We split both sets using 75% for the VLM and the remainder for the classifier. The VLM test set is used for validation since no test set is required here. The classifier training points are split randomly in

a 9:1 ratio to form training and validation sets. We report classifier performance on the classifier test set.

Lending Club: This dataset is split into train, validation and test sets according to the issue date of the loans. The oldest 85% of data forms the training data, with the remaining forming the validation and test data. As with MNIST, we use 75% for the split between VLM training data and classifier training data.

E.1.2. NOVEL-CLASS CLASSIFICATION

MNIST: We use a similar approach to the above, but split the data between the VLM and the classifier such that the VLM train/validation sets contain $\frac{8}{9}$ ths of (unlabelled) training images from classes 0 to 8. The remaining $\frac{1}{9}$ ths of 0 to 8 images, and all 9s, are used for classifier train, test and validation sets. Our VLM datasets then contain equal class balance for the classes 0 to 8, and the classifier datasets contain equal class balance for 9s and ‘not 9s’.

E.1.3. DATA JOIN

Lending Club: For this experiment, the datasets were split column-wise, between the dataset’s 23 features, such that 8 features remained clean (month of earliest credit line, number of open credit lines, initial listing status of loan, application type, address (US state), home ownership status, employment length, public record bankruptcies) and the remaining 15 features were privatized. The feature split was chosen such that the 8 clean features contain some information to solve the classification task, while the remaining 15 features contain information which, at least before privatization, further improves classifier performance.

E.2. Noising Features Directly

For the Laplace mechanism, we assume that Δf is equal to the difference between the maximum and minimum value of the (continuous) feature within the training and validation sets used to train the VLM in the main experiments, after pre-processing. One then has to clip any values that lie outside this interval in the shared/collected dataset at privatization time.

For Wang et al. (2019)’s mechanism, we map all continuous features to $[-1, 1]$ before applying the mechanism.

E.3. Hyperparameter Choices

We conducted a grid search over a number of the hyperparameters in our model, in order to find the optimal experimental setup.

For stage 1 of the VLM training, a learning rate of 10^{-4} and batch size of 128 was used for Lending Club experiments, and a learning rate of 5×10^{-4} and batch size of 64

was used for MNIST. We then searched over the following model hyperparameters (with central $\epsilon = \infty$):

- The proportion λ of our privacy budget assigned to the datapoint, compared with the label i.e. $\lambda = \epsilon_x / (\epsilon_x + \epsilon_y)$.
- The ℓ_1 clipping distance l of our inference network mean i.e. $l = \Delta\mu_\phi / 2$.
- The Laplace distribution scale b of our approximate posterior distribution during pre-training of the VLM. Note that we report this as the $\epsilon_{\text{pre-training}}$ -LDP value induced by a sample from this posterior distribution, given l in the previous point i.e. $\epsilon_{\text{pre-training}} = 2l/b$. This is fixed throughout training, unless ‘learned’ is specified in the below table, in which case the parameter b is a learned scalar.
- The latent dimension d . This was fixed to 8 for data collection experiments but we searched over $d \in \{5, 8\}$ for the data join experiments due to the smaller number of features.

We also did a grid search over the following DP-Adam hyperparameters for central $\epsilon \in \{1, 5\}$:

- Noise multiplier
- Batch size
- DP learning rate

The DP-Adam hyperparameter max gradient norm was fixed to 1 throughout. The number of training epochs needed to reach the target central ϵ value follows from the choice of hyperparameters, combined with the VLM training set size (45,000 for MNIST, and 341,000 for Lending Club). Note that we fixed $\delta = 10^{-5}$ for all experiments.

The results from these grid searches are given in Tables 2, 3, and 4.

Table 2. VLM hyperparameters used for data join experiments on the Lending Club dataset.

Local ϵ	d	l	$\epsilon_{\text{pre-training}}$
∞	8	5	20
10	8	5	10
8	5	5	15
6	5	5	15
4	5	5	10
2	5	5	15
1	5	5	10

E.4. Network Architectures

Throughout the paper, we used feedforward architectures for both the VLM and classifier networks.

For MNIST, we use a VLM encoder network with 3 hidden layers of size $\{400, 150, 50\}$, and a decoder network with 3 hidden layers of size $\{50, 150, 400\}$. For Lending Club, we use a VLM encoder and decoder network with 2 hidden layers of size $\{500, 500\}$. For the the latent level classifier we used a network with 1 hidden layer of size 50 and for pixel level classifier we use a network with 3 hidden layers of size $\{400, 150, 50\}$.

F. Proof of Upper Bound on Noisy Accuracy

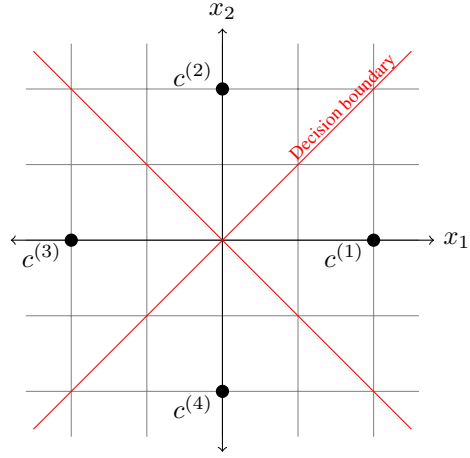


Figure 6. The decision boundary for a classifier that equally separates (in ℓ_1 -distance) vertices $c^{(i)}$ for $i \in \{1, 2, 3, 4\}$ in 2-dimensional space.

In this section, we derive an upper bound on accuracy for the classification of datapoints privatized using the Laplace mechanism (see Equation 4). To simplify the proof, we make the following assumptions:

- We have K equally balanced classes.
- K is even.
- $K \leq 2d$ where d is the dimension of the output of $f(\cdot)$ (the latent space on which we add Laplace noise).

These are true for all experiments in this paper.

First, suppose that $K = 2d$. Since we add iid Laplace noise to each datapoint, we will obtain the highest possible accuracy when $f(\cdot)$ maps datapoints from class i as far away from datapoints from class $j \neq i$ as possible. This maximum separation distance can be at most Δf ; we can separate all K classes by distance Δf in our d dimensional

Table 3. DP-Adam hyperparameters used for data collection and novel-class classification.

Task	Central ϵ	Learning Rate	Batch Size	Noise Multiplier
MNIST	5	5e-4	64	0.7
	1	5e-4	64	1.1
Lending Club	5	1e-4	128	0.56
	1	1e-4	128	1.1

latent space iff each class is mapped to a separate vertex $c^{(y)}$ of the taxicab sphere of (ℓ_1 -norm) radius $\Delta f/2$.

The decision boundary is given by the line that equally separates these vertices in ℓ_1 -space, as shown (for 2 dimensions) in Figure 6.

The accuracy of the classifier \mathcal{C} on datapoints privatized by the latent-space Laplace mechanism $q(\cdot|x) \sim \text{Laplace}(f(x), \Delta f/\epsilon)$ is given by

$$A = \mathbb{E}_{(x,y) \sim p(x,y), \tilde{z} \sim q(z|x)} p(\mathcal{C}(\tilde{z}) = y) \quad (25)$$

$$= \mathbb{E}_{y \sim p(y)} p(\mathcal{C}(c^{(y)} + s) = y) \quad (26)$$

$$= p(\mathcal{C}(c^{(1)} + s) = 1) \quad (27)$$

where $s = (s_1, \dots, s_d)$ and $s_i \sim \text{Laplace}(0, \Delta f/\epsilon)$. The second equality follows from the fact that all points from a given class are mapped to the same point in latent space, and the final equality follows from the symmetry between classes. This final term gives the probability that when we add Laplace noise to $c^{(1)}$ and obtain the private representation $\tilde{c}^{(1)}$, we do not cross the decision boundary. We assume WLOG that $c^{(1)} = (1, 0, \dots, 0)$ and calculate this probability as follows (dropping the superscript for clarity)

$$A = \int_{\substack{\tilde{c}_1 > 0, \\ \tilde{c}_i < |\tilde{c}_1|, \forall i \neq 1}} d\tilde{c}_{1:d} \frac{1}{(2b)^d} e^{-\frac{||\tilde{c} - c||_1}{b}} \quad (28)$$

$$= \int_0^\infty d\tilde{c}_1 \frac{1}{2b} e^{-\frac{|\tilde{c}_1 - 1|}{b}} \prod_{i=2}^d \int_{-\tilde{c}_1}^{\tilde{c}_1} d\tilde{c}_i \frac{1}{2b} e^{-\frac{|\tilde{c}_i|}{b}} \quad (29)$$

$$= \int_0^\infty d\tilde{c}_1 \frac{1}{2b} e^{-\frac{|\tilde{c}_1 - 1|}{b}} \left(1 - e^{-\tilde{c}_1/b}\right)^{d-1} \quad (30)$$

$$= \int_0^\infty d\tilde{c}_1 \frac{1}{2b} e^{-\frac{|\tilde{c}_1 - 1|}{b}} \sum_{j=0}^{d-1} \binom{d-1}{j} (-1)^j e^{-\frac{j\tilde{c}_1}{b}} \quad (31)$$

$$= \sum_{j=0}^{d-1} \binom{d-1}{j} (-1)^j \int_0^\infty d\tilde{c}_1 \frac{1}{2b} e^{-\frac{|\tilde{c}_1 - 1|}{b}} e^{-\frac{j\tilde{c}_1}{b}} \quad (32)$$

$$= \sum_{j=0}^{d-1} \binom{d-1}{j} (-1)^j \left[\int_0^1 d\tilde{c}_1 \frac{1}{2b} e^{-\frac{\tilde{c}_1(j-1)+1}{b}} \right. \\ \left. + \int_1^\infty d\tilde{c}_1 \frac{1}{2b} e^{-\frac{\tilde{c}_1(j+1)-1}{b}} \right] \quad (33)$$

$$= \frac{1-d}{2b} \left(1 + \frac{b}{2}\right) e^{-1/b} \\ + \sum_{j=0, j \neq 1}^{d-1} \binom{d-1}{j} (-1)^j \left[\frac{e^{-j/b}}{1-j^2} - \frac{e^{-1/b}}{2(1-j)} \right] \quad (34)$$

$$= (1-d) \frac{\epsilon+1}{4} e^{-\epsilon/2} \\ + \sum_{j=0, j \neq 1}^{d-1} \binom{d-1}{j} (-1)^j \left[\frac{e^{-j\epsilon/2}}{1-j^2} - \frac{e^{-\epsilon/2}}{2(1-j)} \right] \quad (35)$$

where in the last step we used the fact that in this case $\epsilon = 2/b$. By substituting $d = K/2$, Equation 12 follows directly.

Now, we consider the case $K \leq 2d$. Clearly, the taxicab sphere has more than K vertices, and so classes can occupy different combinations of vertices. The maximum accuracy will be found where the occupied vertices are maximally separated from each other. For the case of Laplace noise, where probability mass decreases exponentially with ℓ_1 -distance from the mean, it is clear that the probability of a noised datapoint crossing a decision boundary is higher when the classes are centered on vertices aligned along different axes. We have shown this for $d = 2$ in Figures 7(a) and 7(b), where clearly the probability mass of the blue shaded area for a Laplace distribution with mean $c^{(1)}$ is larger than the green shaded area. Therefore we are more likely to cross the decision boundary in Figure 7(b), given a fixed quantity of noise.

Thus, the optimal setup is when the K classes are positioned on vertices aligned along the first $K/2$ axes. Noise added to the remaining $d - K/2$ dimensions does not affect the classifier, and so Equation 35 still holds.

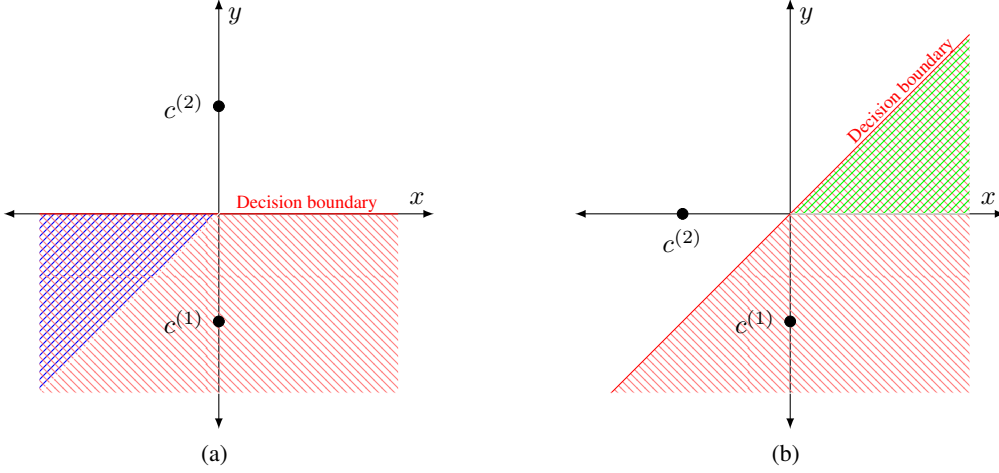


Figure 7. The shaded areas represent, for $d = 2$ and $K = 2$, the decision boundaries for: (a) a function $f(\cdot)$ that maps the two classes onto opposing vertices; (b) a function $f(\cdot)$ that maps the two classes onto adjacent vertices. Refer to Appendix F for details on the color-coding of shaded areas.

G. Feature Level Private Classifier for Data Collection

Figure 8 shows the private accuracy results for MNIST data collection, on latent level.

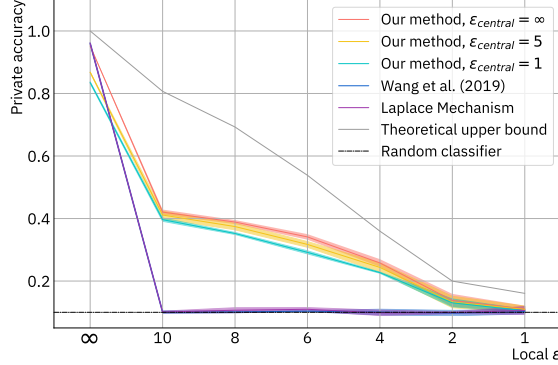


Figure 8. Private accuracy as a function of local ϵ for data collection (feature level). Each line indicates a different value of $(\epsilon, \delta = 10^{-5})$ -CDP at which the encoder was trained, each point on the x -axis shows the ϵ -LDP guarantee for the collected training set.

Table 4. VLM hyperparameters used for data collection and novel-class classification.

Experiment	Task	Local ϵ	λ	l	$\epsilon_{\text{pre-training}}$																																																																														
Clean Accuracy, Latent Level Classification	MNIST	∞	N/A	10	learned																																																																														
		10	0.7	10	27																																																																														
		8	0.7	5	29																																																																														
		6	0.7	5	15																																																																														
		4	0.7	7.5	5																																																																														
		2	0.7	7.5	21																																																																														
		1	0.7	5	15																																																																														
		∞	N/A	10	learned																																																																														
		10	0.7	5	15																																																																														
		8	0.7	5.	29																																																																														
Private Accuracy, Latent Level Classification	Lending Club	6	0.7	5.	29																																																																														
		4	0.7	5	15																																																																														
		2	0.95	5	15																																																																														
		1	0.95	10	21																																																																														
		∞	N/A	10	learned																																																																														
		10	0.95	5	15																																																																														
		8	0.95	5.	15																																																																														
		6	0.7	5.	15																																																																														
		4	0.7	5	15																																																																														
		2	0.95	5	29																																																																														
Clean Accuracy, Feature Level Classification	MNIST	1	0.95	10	21																																																																														
		∞	N/A	10	learned																																																																														
		10	0.7	5	29																																																																														
		8	0.7	5	15																																																																														
		6	0.7	7.5	21																																																																														
		4	0.7	5	5																																																																														
		2	0.7	7.5	5																																																																														
		1	0.7	5	15																																																																														
		∞	N/A	10	learned																																																																														
		10	0.7	5	29																																																																														
Private Accuracy, Feature Level Classification	Lending Club	8	0.95	5.	29																																																																														
		6	0.7	5.	15																																																																														
		4	0.7	5	15																																																																														
		2	0.7	5	15																																																																														
		1	0.7	10	15																																																																														
		∞	N/A	10	learned																																																																														
		10	0.7	5	5																																																																														
		8	0.7	10	5																																																																														
		6	0.7	10	5																																																																														
		4	0.7	5	5																																																																														
Clean Accuracy, Feature Level Classification	MNIST	2	0.7	7.5	5	1	0.95	5	15	∞	N/A	10	learned	10	0.95	5	15	8	0.95	5.	15	6	0.95	5.	15	4	0.7	5	15	2	0.95	7.5	27	1	0.95	5	15	∞	N/A	10	learned	Private Accuracy, Feature Level Classification	Lending Club	10	0.95	5	15	8	0.95	5.	15	6	0.95	5.	15	4	0.7	5	15	2	0.95	7.5	27	1	0.95	5	15	∞	N/A	10	learned	10	0.95	5	15	8	0.95	5.	15	6	0.95	5.	15
		2	0.7	7.5	5																																																																														
		1	0.95	5	15																																																																														
		∞	N/A	10	learned																																																																														
		10	0.95	5	15																																																																														
		8	0.95	5.	15																																																																														
		6	0.95	5.	15																																																																														
		4	0.7	5	15																																																																														
		2	0.95	7.5	27																																																																														
		1	0.95	5	15																																																																														
		∞	N/A	10	learned																																																																														
Private Accuracy, Feature Level Classification	Lending Club	10	0.95	5	15	8	0.95	5.	15	6	0.95	5.	15	4	0.7	5	15	2	0.95	7.5	27	1	0.95	5	15	∞	N/A	10	learned	10	0.95	5	15	8	0.95	5.	15	6	0.95	5.	15																																										
		10	0.95	5	15																																																																														
		8	0.95	5.	15																																																																														
		6	0.95	5.	15																																																																														
		4	0.7	5	15																																																																														
		2	0.95	7.5	27																																																																														
		1	0.95	5	15																																																																														
		∞	N/A	10	learned																																																																														
		10	0.95	5	15																																																																														
		8	0.95	5.	15																																																																														
		6	0.95	5.	15																																																																														